Latin American Journal of Solids and Structures
www.lajss.org

An Accurate Study on Capacitive Microphone with Circular Diaphragm Using a Higher Order Elasticity Theory

Abstract

This study has been undertaken to investigate the mechanical behavior of the capacitive microphone with clamped circular diaphragm using modified couple stress theory in comparison to the classical one. Presence of the length scale parameter in modified couple stress theory provides the means to evaluate the size effect on the microphone mechanical behavior. Investigating Pull-in phenomenon and dynamic behavior of the microphone are the matters provided due to the application of a step DC voltage. Also the effects of different air damping coefficients on dynamic pull-in voltage and pull-in time have been studied. The output level or sensitivity of the microphone has been studied by investigating the frequency response in term of magnitude for different length scale parameters to figure out how the length scale parameter affects on the sensitivity of the capacitive microphone.

To achieve these ends, the nonlinear differential equation of the circular diaphragm has been extracted using Kirchhoff thin plate theory. Then, a Step-by-Step Linearization Method (SSLM) has been used to escape from the nonlinearity of the differential equation. Afterwards, Galerkin-based reduced-order model has been applied to solve the obtained equation.

Keywords

MEMS, capacitive microphone, couple stress theory, length scale parameter, sensitivity.

Shakiba Dowlati [a]
Ghader Rezazadeh [b*]
Saeid Afrang [a]
Mehrdad Sheykhlou [b]
Aysan Madan Pasandi [a]

[a] Electrical Engineering Department, Urmia University, Iran
[b] Mechanical Engineering Department, Urmia University, Iran

[*]Author email: g.rezazadeh@urmia.ac.ir

http://dx.doi.org/10.1590/1679-78252268

Received 02.07.2015
In revised form 18.11.2015
Accepted 20.11.2015
Available online 05.01.2016

1 INTRODUCTION

A microphone is an electro-acoustic transducer that converts the acoustic energy into electrical signals. The microphones are broadly utilized in voice communications devices, hearing aids, vibration control and surveillance military aims (Miao et al., 2002; Ma et al., 2002). Traditional microphones suffer from the disadvantages of high cost and large size. Therefore there is a further need to study on technology which can overcome these problems.

Micro-electro-mechanical technology defined as miniaturized mechanical and electro-mechanical elements is going to be more and more convenient in almost all fields of industries (Rezazadeh et al., 2010; Vahdat et al., 2011; Rezazadeh et al., 2012). However, its applications in electronics draw more attention, specifically. Microphones can be mainly categorized into dynamic, optical and capacitor (Suzuki et al., 2006). MEMS-based capacitive microphones are used where low power, low noise level, large band width and high sensitivity are the crucial requirements. In the case of MEMS capacitive microphones a diaphragm movement toward a ground plate is caused by the applied acoustic pressure on the diaphragm leading to a changing capacitance (Kwon et al., 2007). The sensing capacitance is calculated by integration of the diaphragm deflection in respect to the fixed ground-plate (Chen et al., 2008). The change in conductance produces a change in voltage needing to be amplified to obtain a measurable signal.

By applying voltage across the two plates, attractive electrostatic and elastic restoring forces have been induced between them. Both forces are increased by raising voltage until the applied voltage is touched to a critical value, in which the diaphragm collapses on the fixed electrode which means pull-in happens (Batra et al., 2008). The critical voltage associated with this instability is called pull-in voltage (Batra et al., 2006). In some cases, delaying the onset of pull-in instability would be extremely desirable as it is considered as a limiting factor of the functional range of capacitive microphone. Accordingly in the design of electrostatically actuated MEMS microphones, cornerstone is to evaluate the pull-in voltage accurately and adjust the electric load away from the pull-in instability (Abdel-Rahman et al., 2002). Many studies have delved into the pull-in phenomenon (Abdel-Rahman et al., 2002; Tilmans and Legtenberg, 1994).

The acoustic sensitivity of the microphone has been described as the output voltage response to an acoustical pressure input (Raichel, 2000). To put it in another word, the mechanical sensitivity is defined as how much the deflection changes per sound pressure applying on the diaphragm (Scheeper et al., 1994). In respect of the same bias voltage and sound pressure, a microphone with a high sensitivity value has a higher output level and needs less preamplifier gain before the analog-to-digital conversion compared to a microphone with a low sensitivity value. A microphone with high sensitivity would be suitable in far-field applications where there is a large distance from the source of sound to the microphone for instance conference phones and security cameras. Li et al. (2001) developed a MEMS capacitor microphone to raise the mechanical sensitivity over releasing the initial stress and diminishing the mechanical stiffness of the diaphragm over a deeply corrugated diaphragm. Also several investigations have looked into the mechanical behavior of MEMS microphone; Quaegebeur and Chaigne (2008) studied effects of mechanical and electrical nonlinearity on the electroacoustical behavior of electrodynamic transducers.

It is perceived from hybrid atomistic-continuum model and experimental results, there is a size effect in micron and sub-micron scales which has a key role in mechanical behavior of microstructures (Tsiatas, 2009). It maintains that the classical theory of elasticity does not touch the accurate and definite characterization of deformation occurrence due to not including Size effect. To overcome this inadequacy and predict the accurate behaviors of microstructures, non-classical theories such as strain gradient theories (Lazopoulos, 2004; Lazopoulos, 2009) nonlocal elasticity theories (Eringen, 1983; Reddy, 2010) and couple stress theories (Toupin, 1962; Mindlin and Tiersten, 1962; Koiter, 1969; Yang et al., 2002) which take the size effect into consideration using length scale pa-

rameters have been applied to develop the non-classical models. The classical couple stress theory was originated by the Cosserat brothers (1909), Toupin (1962), Mindlin and Tiersten (1962), and Koiter (1969) to delve into the size-dependent behavior of microstructures. They utilized two length scale parameters to capture the size effects. Yang et al. (2002) developed an additional equilibrium relation assuming the couple stress tensor to be symmetric. This work led to the number reduction of material length scale parameter from the two in classical couple stress theory to only one, established in the modified couple stress theory (MCST). The two main advantageous which make the MCST more preferable over the classical couple stress theory are using only one length scale parameter besides Lame's constants and symmetry of couple stress tensor (Park and Gao, 2006; Ma et al., 2008). The vast majority of the studies around the microphones are restricted to the classical theory (CT) which have not been associated with material length scale parameter therefore they may lead to the inaccurate predictions of the mechanical behavior. Accordingly, using non-classical theories is inevitable for approaching the more accurate mechanical behavior of these devices.

This paper aims to carry out the instability behavior and the sensitivity of the capacitive microphone exposed to an electrostatic force based on the MCST for various material length scale parameters and compared with the CT. In addition the effect of various damping coefficients on dynamic behavior is investigated. The differential equations of microphone are formulated by a Kirchhoff thin plate theory applying MCST. A step-by-step linearization method (SSLM), and the Galerkin based reduced order model are used for evaluation of the mechanical behavior of microphone.

2 MECHANICAL MODEL AND GOVERNING EQUATIONS

2.1 The Modeling of System

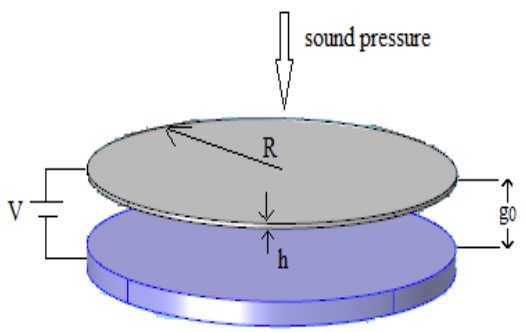

Figure 1: Schematic illustration of the capacitive microphone with electrostatic actuation.

A MEMS capacitive microphone generally can be viewed as two conductive circular micro plate with a voltage across them as illustrated in figure 1 The top plate is a thin deformable elastic plate with thickness h $(-h/2 \leq z \leq h/2)$, radius R $(-R \leq r \leq R)$, Poisson's ratio ν and young's modulus E which is held fixed along its boundary and plays the role of diaphragm. According to low weight of the diaphragm, it can vibrate back and forth and produce energy. The lower plate of the

capacitor is fixed, rigid and thick with no movement introduces as the reference. These two plates are separated by a dielectric substance like air.

Applying a DC voltage to microphone causes an electrostatic pull down force that can be represented as follows:

$$F(w,V) = \frac{\varepsilon_0 V^2}{2(g_0 - w(r,\theta))^2} \tag{1}$$

Where ε_0 is the dielectric constant of the air, V is the applied bias DC voltage, g_0 is the initial gap between the diaphragm and the back plate, t is the time and $w(r,\theta)$ is the deflection of the diaphragm. A change in the distance of upper and lower plates owing to electrostatic pull-down force leads to the capacitance value changing. Thus the structure acts as a variable capacitor.

The air pressure changes constantly with time, but at a certain point of time it has an exact value. A sound pressure wave can be represented by a random time dependent mathematical function with a wide range of frequencies approximated by Fourier series as a combination of simple sinusoidal functions. In this paper, we consider a pure sinusoidal sound wave as the actuation source of the microphone as follows:

$$P(\omega_s,t) = P_0 \sin(\omega_s t) \tag{2}$$

In which P_0 and ω_s are the amplitude and frequency of the sound pressure wave, respectively. During the diaphragm oscillation normally to the substrate, the air gap is squeezed leading to a considerable change in the air volume. Owing to the viscous flow of air and so does the pressure changing, types of forces are come into existence. One is the restoring force known as air spring caused by the air compression. The total stiffness of the system is given by the rigidity of the diaphragm and the spring effect of the air gap. In the audio frequency range, the air gap spring coefficient is very low comparing to the diaphragm spring coefficient. Therefore, the air gap stiffness can be neglected (Esteves et al., 2011). The other one is damping force caused by the viscous flow of the air which is effective in the microphone operation, particularly in the high frequencies (Esteves et al., 2011). A circular plate damping coefficient is described as follows by analytically solving the Reynolds equation (Bao and Yeng, 2007).

$$C = \frac{3}{2\pi g^3}\eta S^2 \tag{3}$$

Where S is the plate area and g is the air gap between the two plates and η is the air viscosity in the ambient conditions. A simple model (Whelan and Hodgon, 1978) as $\eta = \rho_a \tilde{v}\lambda / 3$ can determine the air viscosity in which ρ_a is the mass density of air, λ is the mean free path of the molecules and $\tilde{v}$ is the average velocity of the molecules. Based on experimental results, different amounts of the air viscosity are derived from ambient conditions including pressure and temperature.

Also during the deflection, the diaphragm carries a certain amount of the fluid volume along itself. This entrained fluid is called added or virtual mass. On the subject of microphone, the virtual

mass and the inertia effect are often neglected since the displaced fluid mass is negligible (De Silva, 2005).

2.2 Modified Couple Stress Formulations

With reference to the modified couple stress theory introduced by Yang et al. (2002), in an isotropic elastic material occupying a volume of Ω bounded by the surface A, the strain energy density is a function of strain and gradient of the rotation vector as following:

$$\prod = \frac{1}{2}\int_{\Omega}(\sigma_{ij} : \varepsilon_{ij} + m_{ji} : \chi_{ji})d\Omega \tag{4}$$

Where σ_{ij} is the Cauchy (classical) stress tensor, ε_{ij} is the strain tensor, m_{ij} is the deviatoric part of the symmetric couple stress tensor, and χ_{ij} is the symmetric curvature tensor as given:

$$\begin{aligned} \sigma_{ij} &= \lambda\varepsilon_{kk}\delta_{ij} + 2\mu\varepsilon_{ij} \\ \varepsilon_{ij} &= \frac{1}{2}(u_{i,j} + u_{j,i}) \\ m_{ij} &= 2\mu\ell^2\chi_{ij} \\ \chi_{ij} &= \frac{1}{2}(\theta_{i,j} + \theta_{j,i}) \end{aligned} \tag{5}$$

In which λ and μ are lame's constants, δ_{ij} is the kronecker delta, u_i is the displacement vector, ℓ is a material inertial length-scale parameter and the parameter θ_i is the rotation vector defined as follow (Yang et al. 2002)

$$\theta_i = \frac{1}{2}\varepsilon_{ijk}u_{k,j} \quad \mu = \frac{E}{2(1+\nu)} \quad \lambda = \frac{E}{(1+\nu)(1-2\nu)} \tag{6}$$

Where ε_{ijk} is the permutation symbol.

2.3 Dynamic Model of a Micro-circular Diaphragm

The relationship between the displacement components $u\,(r,\theta,\mathrm{z})$, $v\,(r,\theta,\mathrm{z})$ and $w(r,\theta,\mathrm{z})$ along the r, θ and z directions, respectively, based on Kirchhoff thin plate theory can be written as (Sun and Tohmyoh, 2009)

$$\mathrm{u}(r,\theta,z) = -z\frac{\partial w(r,\theta)}{\partial r} \qquad \mathrm{v}(r,\theta,z) = -z\frac{\partial w(r,\theta)}{r\partial\theta} \qquad w(r,\theta,z) = w(r,\theta) \tag{7}$$

Assuming a two-dimensional formulation system by dropping the z dependency the strain and curvature tensor are, respectively, described by:

$$\varepsilon = \begin{bmatrix} \dfrac{\partial u}{\partial r} & \dfrac{1}{2}\left(\dfrac{\partial u}{r\partial\theta}+\dfrac{\partial v}{\partial r}-\dfrac{v}{r}\right) & \dfrac{1}{2}\left(\dfrac{\partial u}{\partial z}+\dfrac{\partial w}{\partial r}\right) \\ \dfrac{1}{2}\left(\dfrac{\partial u}{r\partial\theta}+\dfrac{\partial v}{\partial r}-\dfrac{v}{r}\right) & \dfrac{u}{r}+\dfrac{\partial v}{r\partial\theta} & \dfrac{1}{2}\left(\dfrac{\partial v}{\partial z}+\dfrac{\partial w}{r\partial\theta}\right) \\ \dfrac{1}{2}\left(\dfrac{\partial u}{\partial z}+\dfrac{\partial w}{\partial r}\right) & \dfrac{1}{2}\left(\dfrac{\partial v}{\partial z}+\dfrac{\partial w}{r\partial\theta}\right) & \dfrac{\partial w}{\partial z} \end{bmatrix} = \begin{bmatrix} -z\dfrac{\partial^2 w}{\partial r^2} & -z\dfrac{\partial}{\partial r}\left(\dfrac{\partial w}{r\partial\theta}\right) & \dfrac{1}{2}\dfrac{\partial w}{\partial r} \\ -z\dfrac{\partial}{\partial r}\left(\dfrac{\partial w}{r\partial\theta}\right) & -z\left(\dfrac{\partial w}{r\partial\theta}+\dfrac{\partial^2 w}{r^2\partial\theta^2}\right) & \dfrac{1}{2r}\dfrac{\partial w}{\partial\theta} \\ \dfrac{1}{2}\dfrac{\partial w}{\partial r} & \dfrac{1}{2r}\dfrac{\partial w}{\partial\theta} & 0 \end{bmatrix} \tag{8}$$

$$\chi = \begin{bmatrix} \dfrac{\partial}{\partial r}\left(\dfrac{\partial w}{r\partial\theta}\right) & -\dfrac{1}{r}\dfrac{\partial w}{\partial r}+\dfrac{\partial^2 w}{r^2\partial\theta^2}-\dfrac{\partial^2 w}{\partial r^2} & 0 \\ -\dfrac{1}{r}\dfrac{\partial w}{\partial r}+\dfrac{\partial^2 w}{r^2\partial\theta^2}-\dfrac{\partial^2 w}{\partial r^2} & -\dfrac{1}{r}\dfrac{\partial}{\partial\theta}\left(\dfrac{\partial w}{\partial r}\right) & 0 \\ 0 & 0 & 0 \end{bmatrix} = \begin{bmatrix} -\dfrac{1}{r^2}\dfrac{\partial w}{\partial\theta}+\dfrac{1}{r}\dfrac{\partial^2 w}{\partial r\partial\theta} & -\dfrac{1}{r}\dfrac{\partial w}{\partial r}+\dfrac{\partial^2 w}{r^2\partial\theta^2}-\dfrac{\partial^2 w}{\partial r^2} & 0 \\ -\dfrac{1}{r}\dfrac{\partial w}{\partial r}+\dfrac{\partial^2 w}{r^2\partial\theta^2}-\dfrac{\partial^2 w}{\partial r^2} & -\dfrac{1}{r}\dfrac{\partial^2 w}{\partial r\partial\theta} & 0 \\ 0 & 0 & 0 \end{bmatrix} \tag{9}$$

By substituting of the Lamé constants with the modulus of elasticity E and the Poisson's ratio ν the stress tensor and the couple stress tensor take the following forms, respectively:

$$\sigma = \begin{bmatrix} \dfrac{E}{1-\nu^2}\left(\dfrac{\partial u}{\partial r}+\nu\left(\dfrac{u}{r}+\dfrac{\partial v}{r\partial\theta}\right)\right) & G\left(\dfrac{\partial u}{\partial\theta}+\dfrac{\partial v}{\partial r}\right) & 0 \\ G\left(\dfrac{\partial u}{\partial\theta}+\dfrac{\partial v}{\partial r}\right) & \dfrac{E}{1-\nu^2}\left(\dfrac{u}{r}+\dfrac{\partial v}{r\partial\theta}+\nu\dfrac{\partial u}{\partial r}\right) & 0 \\ 0 & 0 & 0 \end{bmatrix} = \begin{bmatrix} \dfrac{-E}{1-\nu^2}\left(z\dfrac{\partial^2 w}{\partial r^2}+\nu z\left(\dfrac{1}{r}\dfrac{\partial w}{\partial r}+\dfrac{1}{r^2}\dfrac{\partial^2 w}{\partial\theta^2}\right)\right) & -2G\ z\dfrac{\partial}{\partial r}\left(\dfrac{1}{r}\dfrac{\partial w}{\partial\theta}\right) & 0 \\ -2G\ z\dfrac{\partial}{\partial r}\left(\dfrac{1}{r}\dfrac{\partial w}{\partial\theta}\right) & \dfrac{-Ez}{1-\nu^2}\left(z\left(\dfrac{1}{r}\dfrac{\partial w}{\partial r}+\dfrac{1}{r^2}\dfrac{\partial^2 w}{\partial\theta^2}\right)+\nu z\dfrac{\partial^2 w}{\partial r^2}\right) & 0 \\ 0 & 0 & 0 \end{bmatrix} \tag{10}$$

$$m = \begin{bmatrix} 2G\ell^2 \dfrac{\partial}{\partial r}\left(\dfrac{1}{r}\dfrac{\partial w}{\partial \theta}\right) & -2G\ell^2\left(\dfrac{1}{r}\dfrac{\partial w}{\partial r} - \dfrac{1}{r^2}\dfrac{\partial^2 w}{\partial \theta^2} + \dfrac{\partial^2 w}{\partial r^2}\right) & 0 \\ -2G\ell^2\left(\dfrac{1}{r}\dfrac{\partial w}{\partial r} - \dfrac{1}{r^2}\dfrac{\partial^2 w}{\partial \theta^2} + \dfrac{\partial^2 w}{\partial r^2}\right) & -2G\ell^2 \dfrac{1}{r}\dfrac{\partial}{\partial \theta}\left(\dfrac{\partial w}{\partial r}\right) & 0 \\ 0 & 0 & 0 \end{bmatrix} \tag{11}$$

In which $G = E \,/\, 2(1+\nu)$ is the shear modulus.

$$M^{\sigma} = \int_{-h/2}^{+h/2} \begin{bmatrix} -\dfrac{Ez}{1-\nu^2}\dfrac{\partial^2 w}{\partial r^2} + \nu z\left(\dfrac{1}{r}\dfrac{\partial w}{\partial r} + \dfrac{1}{r^2}\dfrac{\partial^2 w}{\partial \theta^2}\right) & -2Gz\dfrac{\partial}{\partial r}\left(\dfrac{1}{r}\dfrac{\partial w}{\partial \theta}\right) & 0 \\ -2Gz\dfrac{\partial}{\partial r}\left(\dfrac{1}{r}\dfrac{\partial w}{\partial \theta}\right) & -\dfrac{Ez}{1-\nu^2}\left(\dfrac{1}{r}\dfrac{\partial w}{\partial r} + \dfrac{1}{r^2}\dfrac{\partial^2 w}{\partial \theta^2}\right) + \nu z\dfrac{\partial^2 w}{\partial r^2} & 0 \\ 0 & 0 & 0 \end{bmatrix} z dz =$$

$$\begin{bmatrix} -D\left[\dfrac{\partial^2 w}{\partial r^2} + \nu\left(\dfrac{1}{r}\dfrac{\partial w}{\partial r} + \dfrac{1}{r^2}\dfrac{\partial^2 w}{\partial r^2}\right)\right] & -D(1-\nu)\dfrac{\partial}{\partial r}\left(\dfrac{1}{r}\dfrac{\partial w}{\partial \theta}\right) & 0 \\ -D(1-\nu)\dfrac{\partial}{\partial r}\left(\dfrac{1}{r}\dfrac{\partial w}{\partial \theta}\right) & -D\left[\left(\dfrac{1}{r}\dfrac{\partial w}{\partial r} + \dfrac{1}{r^2}\dfrac{\partial^2 w}{\partial r^2}\right) + \nu\dfrac{\partial^2 w}{\partial r^2}\right] & 0 \\ 0 & 0 & 0 \end{bmatrix} \tag{12}$$

$$M^{m} = \int_{-h/2}^{+h/2} \begin{bmatrix} 2G\ell^2 \dfrac{\partial}{\partial r}\left(\dfrac{1}{r}\dfrac{\partial w}{\partial \theta}\right) & -2G\ell^2\left(\dfrac{1}{r}\dfrac{\partial w}{\partial r} - \dfrac{1}{r^2}\dfrac{\partial^2 w}{\partial \theta^2} + \dfrac{\partial^2 w}{\partial r^2}\right) & 0 \\ -2G\ell^2\left(\dfrac{1}{r}\dfrac{\partial w}{\partial r} - \dfrac{1}{r^2}\dfrac{\partial^2 w}{\partial \theta^2} + \dfrac{\partial^2 w}{\partial r^2}\right) & -2G\ell^2 \dfrac{1}{r}\dfrac{\partial}{\partial \theta}\left(\dfrac{\partial w}{\partial r}\right) & 0 \\ 0 & 0 & 0 \end{bmatrix} dz =$$

$$\begin{bmatrix} 2D^{\ell} \dfrac{\partial}{\partial r}\left(\dfrac{1}{r}\dfrac{\partial w}{\partial \theta}\right) & -2D^{\ell}\left(\dfrac{1}{r}\dfrac{\partial w}{\partial r} - \dfrac{1}{r^2}\dfrac{\partial^2 w}{\partial \theta^2} + \dfrac{\partial^2 w}{\partial r^2}\right) & 0 \\ -2D^{\ell}\left(\dfrac{1}{r}\dfrac{\partial w}{\partial r} - \dfrac{1}{r^2}\dfrac{\partial^2 w}{\partial \theta^2} + \dfrac{\partial^2 w^2}{\partial r^2}\right) & -2D^{\ell}\dfrac{1}{r}\dfrac{\partial}{\partial \theta}\left(\dfrac{\partial w}{\partial r}\right) & 0 \\ 0 & 0 & 0 \end{bmatrix} \tag{13}$$

Where $D = Eh^3 \,/\, 12(1-\nu^2)$ is the bending rigidity of the diaphragm and $D^l = El^2 h \,/\, 2(1+\nu) = Gl^2 h$ is the contribution of rotation gradients to the bending rigidity.

According to Hamilton's principle, the actual motion diminishes the difference between the kinetic energy and total potential energy for a system with prescribed configurations at $t = 0$ to T as follows (Reddy, 2002):

$$\int_0^T \left[\delta K - (\delta \prod - \delta W)\right] dt = 0 \tag{14}$$

Where k, Π and W are the kinetic energy, the strain energy and the work of external loads of the micro plate, respectively.

The strain energy density can be obtained from eqs. (4), (12) and (13) as follows:

$$\prod = \frac{1}{2}\int_A \left\{ \begin{array}{l} -M_{rr}^{\sigma}\dfrac{\partial^2 w}{\partial r^2} - M_{\theta\theta}^{\sigma}\left(\dfrac{1}{r}\dfrac{\partial w}{\partial r} + \dfrac{1}{r^2}\dfrac{\partial^2 w}{\partial \theta^2}\right) \\ -2M_{r\theta}^{\sigma}\dfrac{\partial}{\partial r}\left(\dfrac{1}{r}\dfrac{\partial w}{\partial \theta}\right) + M_{rr}^{m}\dfrac{\partial}{\partial r}\left(\dfrac{1}{r}\dfrac{\partial w}{\partial \theta}\right) \\ -M_{\theta\theta}^{m}\dfrac{\partial}{\partial \theta}\left(\dfrac{1}{r}\dfrac{\partial w}{\partial r}\right) - M_{r\theta}^{m}\left(\dfrac{1}{r}\dfrac{\partial w}{\partial r} - \dfrac{1}{r^2}\dfrac{\partial^2 w}{\partial \theta^2} + \dfrac{\partial^2 w}{\partial r^2}\right) \end{array} \right\} dA \tag{15}$$

Moreover, the first variation of the strain energy in the plate on the time interval [0, T] can be expressed as:

$$\delta\int_0^T \prod dt = \int_0^T \int_A \left\{ \begin{array}{l} -\dfrac{\partial^2 M_{rr}^{\sigma}}{\partial r^2} - \dfrac{2}{r}\dfrac{\partial M_{rr}^{\sigma}}{\partial r} - \dfrac{1}{r^2}\dfrac{\partial^2 M_{\theta\theta}^{\sigma}}{\partial \theta^2} + \dfrac{1}{r}\dfrac{\partial M_{\theta\theta}^{\sigma}}{\partial r} - \dfrac{2}{r}\dfrac{\partial^2 M_{r\theta}^{\sigma}}{\partial r \partial \theta} \\ -\dfrac{2}{r^2}\dfrac{\partial M_{r\theta}^{\sigma}}{\partial \theta} + \dfrac{1}{r}\dfrac{\partial^2 M_{rr}^{m}}{\partial \theta \partial r} + \dfrac{1}{r^2}\dfrac{\partial M_{rr}^{m}}{\partial \theta} - \dfrac{1}{r}\dfrac{\partial^2 M_{\theta\theta}^{m}}{\partial \theta \partial r} \\ +\dfrac{1}{r}\dfrac{\partial M_{r\theta}^{m}}{\partial r} - \dfrac{2}{r}\dfrac{\partial M_{r\theta}^{m}}{\partial r} + \dfrac{1}{r^2}\dfrac{\partial^2 M_{r\theta}^{m}}{\partial \theta^2} - \dfrac{\partial^2 M_{r\theta}^{m}}{\partial r^2} \end{array} \right\} \delta w \, dA \, dt \tag{16}$$

The work done by the external forces can be obtained as:

$$W^{ext} = \int_A \mathrm{Q(r)w(r,t)dA} \tag{17}$$

The first variations of the work on the time interval [0, T] is:

$$\delta\int_0^T W dt = \int_0^T \int_A Q(\mathrm{r}) \delta w \, dA \, dt \tag{18}$$

Total kinetic energy of the circular diaphragm is given by:

$$K = \frac{1}{2}\int_{\Omega} \rho \left[\left(\frac{\partial u}{\partial t}\right)^2 + \left(\frac{\partial v}{\partial t}\right)^2 + \left(\frac{\partial w}{\partial t}\right)^2 \right] d\Omega \tag{19}$$

Where ρ is the mass density of material. Applying $\partial u / \partial t = \partial v / \partial t = 0$ the first variation of total kinetic energy of the plate on the time interval [0, T] takes the form:

$$\delta\int_0^T K dt = -\int_0^T \int_A \rho h \left(\frac{\partial w}{\partial t}\right)^2 \delta w \, dA \, dt \tag{20}$$

Substituting Eqs. (16), (18) and (20) into Eq. (14), the governing equilibrium differential equation of motion of a circular micro plate becomes as:

$$\begin{aligned}&\frac{\partial^2 M_{rr}^{\sigma}}{\partial r^2}+\frac{2}{r}\frac{\partial M_{rr}^{\sigma}}{\partial r}+\frac{1}{r^2}\frac{\partial^2 M_{\theta\theta}^{\sigma}}{\partial \theta^2}-\frac{1}{r}\frac{\partial M_{\theta\theta}^{\sigma}}{\partial r}+\frac{2}{r}\frac{\partial^2 M_{r\theta}^{\sigma}}{\partial r\partial\theta}+\frac{2}{r^2}\frac{\partial M_{r\theta}^{\sigma}}{\partial\theta}-\frac{1}{r}\frac{\partial^2 M_{rr}^{m}}{\partial r\partial\theta}\\&-\frac{1}{r^2}\frac{\partial M_{rr}^{m}}{\partial\theta}+\frac{1}{r}\frac{\partial^2 M_{\theta\theta}^{m}}{\partial r\partial\theta}-\frac{1}{r}\frac{\partial M_{r\theta}^{m}}{\partial r}+\frac{2}{r}\frac{\partial M_{r\theta}^{m}}{\partial r}-\frac{1}{r^2}\frac{\partial^2 M_{r\theta}^{m}}{\partial\theta^2}+\frac{\partial^2 M_{r\theta}^{m}}{\partial r^2}+Q=\rho h\frac{\partial^2 w}{\partial t^2}\end{aligned} \tag{21}$$

Substituting Eqs. (12) and (13) into Eq. (21) the governing equation of the micro-plate in terms of the deflection is given by:

$$(D+D^{\ell})\nabla^4 w+\rho h\frac{\partial^2 w}{\partial t^2}=Q \tag{22}$$

Because it is assumed that the plate deflection is symmetrical with respect to circumferential coordinate $\partial w/\partial\theta=0$, the deflection only depends on the radial position r. Therefore the operations ∇^2 and ∇^4 in polar coordinates system for the axisymmetric circular micro plate are expressed as:

$$\begin{aligned}\nabla^2&=\frac{\partial^2}{\partial r^2}+\frac{1}{r}\frac{\partial}{\partial r}\\\nabla^4&=\left(\frac{\partial^2}{\partial r^2}+\frac{1}{r}\frac{\partial}{\partial r}\right)\left(\frac{\partial^2}{\partial r^2}+\frac{1}{r}\frac{\partial}{\partial r}\right)\end{aligned} \tag{23}$$

Therefore for a circular micro plate actuated by electrostatic force and sound pressure wave considering an equivalent damping ratio, equation of motion takes the following form:

$$(D+D^{\ell})\nabla^4 w+\rho h\frac{\partial^2 w}{\partial t^2}+C\frac{\partial w}{\partial t}=\frac{\varepsilon_0 V^2}{2(g_0-w)^2}+P_0\sin(\omega_s t) \tag{24}$$

For convenience the below non-dimensional parameters are presented in order to rearrange the equation into dimensionless form:

$$\hat{w}=\frac{w}{g_0},\hat{r}=\frac{r}{R},\hat{t}=\frac{t}{t^*},\hat{\omega}_s=\frac{\omega_s}{\omega_s^*},t^*=R^2\sqrt{\frac{\rho h}{D}},{\omega_s}^*=\frac{1}{t^*} \tag{25}$$

$$\left(\frac{D+D^{\ell}}{D}\right)\nabla^4\hat{w}+\frac{\partial^2\hat{w}}{\partial\hat{t}^2}+\alpha_3\frac{\partial\hat{w}}{\partial\hat{t}}=\frac{\alpha_1 V^2}{(1-\hat{w})^2}+\alpha_2\sin(\omega_s t) \tag{26}$$

$$\alpha_1=\frac{\varepsilon_0 R^4}{2D{g_0}^3}\quad\alpha_2=\frac{P_0 R^4}{Dg_0}\quad\alpha_3=\frac{CR^4}{Dt^*} \tag{27}$$

3 NUMERICAL SOLUTION

3.1 Nonlinear Equation of Static Deflection

Due to the non-linearity of static deflection of the diaphragm subjected to an applied DC voltage, an analytical solution is complicated and time consuming. Therefore, SSLM is used (Rezazadeh et al., 2009) to linearize the static motion equation.

Assuming that $\mathrm{w^i}$ is the diaphragm deflection due to applied DC voltage $\mathrm{V^i}$:

$$\left(\frac{D+D^{\ell}}{D}\right)\nabla^4 \hat{w}_s^{\,i} = \alpha_1 \frac{(V^i)^2}{(1-\hat{w}_s^{\,i})^2} \tag{28}$$

By increasing the applied DC voltage to:

$$V^{i+1} \rightarrow V^i + \delta V \tag{29}$$

The displacement can be written as:

$$\hat{w}_s^{i+1} \rightarrow \hat{w}_s^i + \psi(\hat{r}) \tag{30}$$

Rewriting Eq. (28) at the step of $(\mathrm{i}+1)$, using the calculus of variation theory and Taylor expansion, neglecting the higher order terms of Taylor series, and subtracting the step (i) from step $(\mathrm{i}+1)$ lead to the following linearized equation to calculate $\psi(\hat{r})$:

$$\left(\frac{D+D^{\ell}}{D}\right)\nabla^4 \psi(\hat{r}) - 2\alpha_1 \frac{(V^{i+1})^2}{(1-\hat{w}_s^i)^3}\psi(\hat{r}) = 2\alpha_1 \frac{V^{i+1}\delta V}{(1-\hat{w}_s^i)^2} \tag{31}$$

$\psi(\hat{r})$ can be approximated by the function space in terms of basis function as follows:

$$\psi_m(\hat{r}) = \sum_{m=1}^{N} a_m \phi_m(\hat{r}) \tag{32}$$

Where $\phi_m(\hat{r})$ is the shape function satisfying the boundary conditions and a_m are the unknown Coefficients evaluated using Galerkin Weighed Residual Method in each step.

Substituting Eq. (32) into Eq. (31), multiplying by the weight function $\phi_k(\hat{r})$ in Galerkin method and then integrating the result with respect to r over [0, 1], lead to a set of differential equation as follows:

$$\sum_{m=1}^{N}(K_{km})a_m = N_k \qquad k = 1,\ldots,N \tag{33}$$

In which

$$K_k = \int_0^1 \left(\left(\frac{D + D^\ell}{D} \right) \nabla^4 \phi_m(\hat{r}) \phi_k(\hat{r}) - \frac{2\alpha_1 V^2}{(1 - \hat{w}_s)^3} \phi_m(\hat{r}) \phi_k(\hat{r}) \right) d\hat{r}$$
$$N_k = \int_0^1 \frac{2\alpha_1 V^i \delta V}{(1 - \hat{w}_s)^2} \phi_k(\hat{r}) d\hat{r} \tag{34}$$

Repeating these steps leads to the deflection of the diaphragm to an applied electrostatic force.

3.2 Nonlinear Equation of Dynamic Deflection

Toward solving Eq. (26) numerically, a Galerkin based model can be used (Nayfeh and Mook, 1979). The approximated solution for solving the dynamic equation of diaphragm deflection is proposed as:

$$w_d(\hat{r}, \hat{t}) = \sum_{n=1}^{N} b_n(\hat{t}) \phi_n(\hat{r}) \tag{35}$$

In which a linear combination of time $b_n(\hat{t})$ and shape function $\phi_n(\hat{r})$ are used. The considered shape function satisfied all boundary conditions of the clamped circular diaphragm.

Substituting Eq. (35) in Eq. (26) leads to following error function:

$$\left(\frac{D + D^\ell}{D} \right) \sum_{n=1}^{N} \nabla^4 \phi_n(\hat{r}) b_n + \alpha_3 \sum_{n=1}^{N} \phi_n(\hat{r}) \dot{b}_n + \sum_{n=1}^{N} \phi_n(\hat{r}) \ddot{b}_n - f(\hat{t}, \hat{w}, \mathrm{V}, \hat{\omega}_s) = E_r \tag{36}$$

Where

$$f(\hat{t}, \hat{w}, V, \hat{\omega}_s) = \frac{2\alpha_1 V^2}{(1 - \hat{w})^2} + \alpha_2 \sin(\hat{\omega}_s \hat{t}) \tag{37}$$

Based on Galerkin method:

$$\int_0^1 \phi_j(\hat{r}) E_r(\hat{r}, \hat{t}) d\hat{r} = 0 \qquad j = 1, \ldots, N \tag{38}$$

Using the weight function $\phi_j(\hat{\mathrm{r}})$ similar to the shape function and applying Galerkin procedure to E_r lead to the following ordinary differential equation:

$$\sum_{n=1}^{N} \left(M_{jn} \ddot{b}_n + C_{jn} \dot{b}_n + K_{jn} b_n \right) = F_j(\hat{\omega}_s, \hat{t}) \qquad j = 1, \ldots, N \ \left(M\ddot{b} + C\dot{b} + kb = F \right) \tag{39}$$

In which

$$
\begin{aligned}
M_{jn} &= \int_0^1 \phi_j(\hat{r})\phi_n(\hat{r})d\hat{r} \\
C_{jn} &= \alpha_3 \int_0^1 \phi_j(\hat{r})\phi_n(\hat{r})d\hat{r} \\
K_{jn} &= \int_0^1 \phi_j(\hat{r}) \left(\left(\frac{D + D^{\ell}}{D} \right) \nabla^4 \phi_n(\hat{r}) - \frac{2\alpha_1 V^2}{\left(1 - \hat{w}_s\right)^3} \phi_n(\hat{r}) \right) d\hat{r} \\
F_j &= \alpha_2 \int_0^1 \phi_j(\hat{r})d\hat{r}
\end{aligned}
\tag{40}
$$

4 NUMERICAL RESULTS AND DISCUSSION

Owing to study the mechanical behavior of microphone including a clamped circular diaphragm with electrostatic actuation, we consider a case with the material and assigned geometrical properties as illustrated in table 1.

In the case of circular diaphragm, the following shape function can be utilized satisfying all boundary conditions.

$$\phi(\hat{r}) = cos^2\left(\frac{(2n-1)\pi}{2}\hat{r}\right) \tag{41}$$

As noted before to evaluate the size effects, an intrinsic material length scale parameter must be incorporate into the constitutive equations. This paper is concerned with three different material length scale parameters as $0.1\,\mu m$, $0.47\,\mu m$ and $0.73\,\mu m$. The ℓ of 0.1 (Bin and Wanji, 2010) refers to a microphone with aluminum diaphragm (Ganji and Majlis, 2008) and the two other length scale parameters belong to a gold diaphragm microphones (Kim et al., 2007) with thickness of 0.5 and 1μm respectively (Cao et al., 2007).

Design variable	Value
R (μm)	250
g_0 (μm)	3
h (μm)	1
E (GPa)	169
ρ (Kg/m^3)	2330
ε_0 (F/m)	8.8541875*10^{-12}
ν	0.3

Table 1: Material properties and geometrical of the diaphragm.

4.1 Stable Region of the Microphone to a DC Voltage

Applying the bias DC voltage to a capacitive microphone reduces the stiffness of the diaphragm, causing the diaphragm to be deflected. By approaching the bias voltage to the static pull-in voltage,

the diaphragm becomes unstable for any initial condition and collapses on the substrate. Considering that this voltage limits the range of the applied DC voltage to the microphone the evaluation of static pull-in voltage is necessary. Figure 2 illustrates the diaphragm non-dimensional center deflection versus voltage using MCST for different length scale parameters. The calculated static pull-in voltage based on MCST is more than the one calculated by CT and increasing the length scale parameter leads to increment of the static pull-in voltage. Results imply that the static pull-in voltage of micron scale diaphragm is size dependent. Also the achieved pull-in voltage under the classical theory ($\ell = 0$) is close to that calculated by Osterboerg (1995).

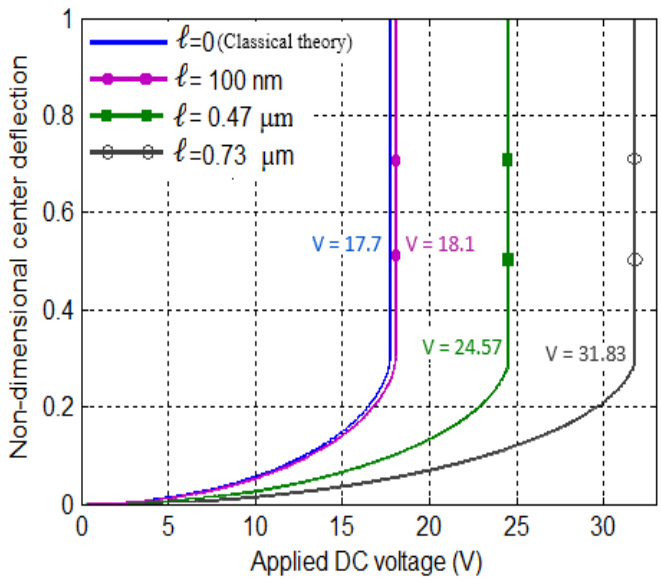

Figure 2: The static pull-in variations based on modified couple stress theory for different length scale parameters in comparison to the classical theory.

4.2 Dynamic Response of the Microphone to a Step DC Voltage ($V_{dc}\neq 0$; $P_0=0$)

The threshold of the step DC voltage applied to the capacitive microphone is limited owing to the dynamic pull-in instability phenomenon. This critical voltage which is as low as 90-92% of static pull-in voltage introduced as dynamic pull-in voltage (Nayfeh et al., 2007). The dynamic motion equation is integrated using Runge-kutta fourth-order method by neglecting the sound pressure wave.

Figures 3 and 4 depict the dynamic behavior of the diaphragm using MCST in comparison to CT, for a case without damping. The predicted results by the classical theory is almost equal to those predicted by applying MCST with a nanosized length scale parameter and increasing the length scale parameter makes the more differences between MCST and CT.

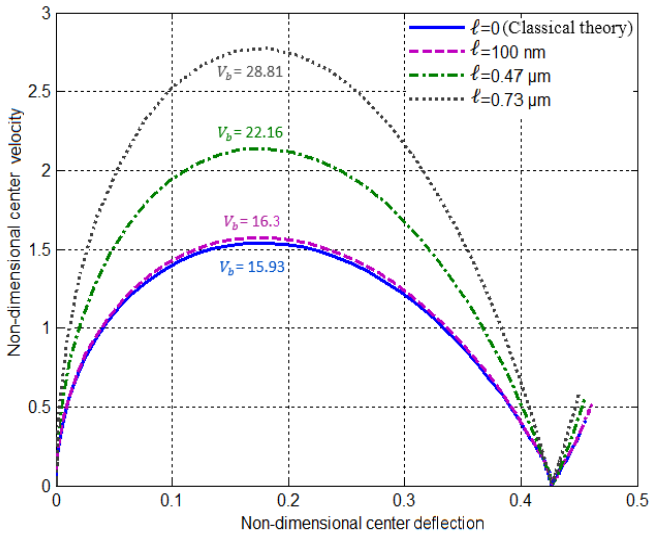

Figure 3: Phase portrait of the diaphragm using modified couple stress theory for different length scale parameters in comparison to the classical theory.

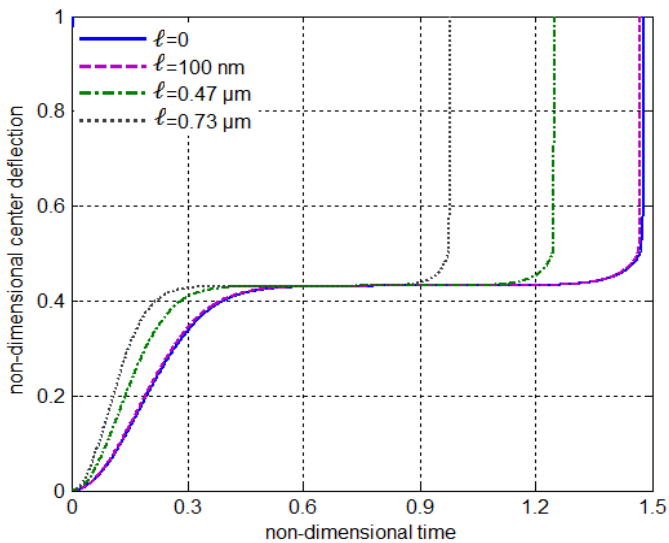

Figure 4: Time history of the diaphragm using modified couple stress theory for different length scale parameters in comparison to the classical theory.

Figures 5 and 6 illustrate the phase portrait and dynamic pull-in variations for different damping coefficients using MCST for $\ell = 0.47\mu m$ in comparison to CT. The small damping ratio refers to the case of larger gap and the lower air viscosity which can be even neglected. Under both theories, increment of the damping coefficient to a critical value causes the dynamic pull-in voltage converges to the static pull-in voltage. As depicted in figure 6, the non-dimensional pull-in time increases by increment of damping ratio. Diminishing the air gap and increasing the air viscosity and plate radi-

us may result in higher damping ratio which causes inappropriate and impractical conditions of using microphone.

Figure 7 shows pull-in time over the applied voltage for various length-scale parameters. Also figure 8 depicts the pull-in time over a range of length-scale parameters. As the length-scale parameter increases, the pull-in time decreases.

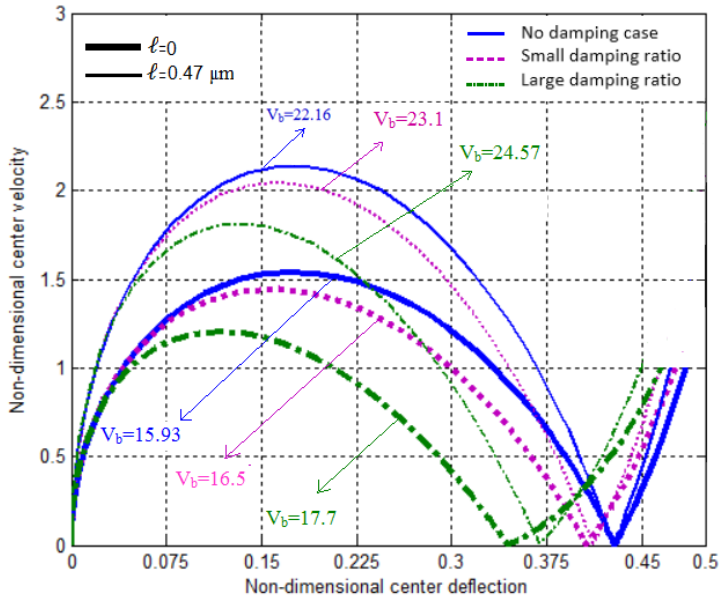

Figure 5: Phase portrait of the diaphragm using modified couple stress theory (ℓ=0.47 μm) for different damping coefficients in comparison to the classical theory.

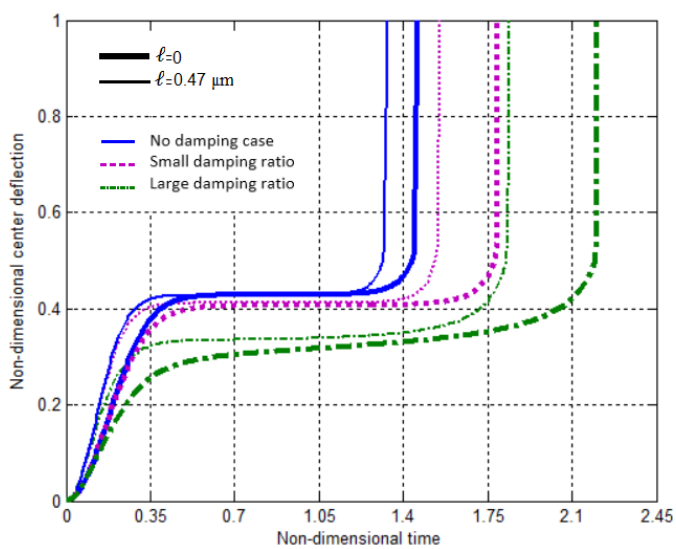

Figure 6: Dynamic pull-in variations of the diaphragm using modified couple stress theory (ℓ=0.47 μm) for different damping coefficients in comparison to the classical theory.

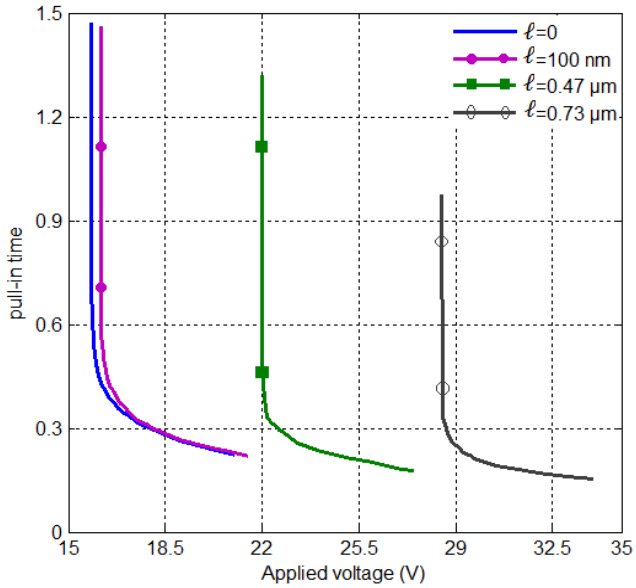

Figure 7: Pull-in time of the diaphragm subjected to the actuating step DC voltage for different length scale parameters in comparison to the classical theory.

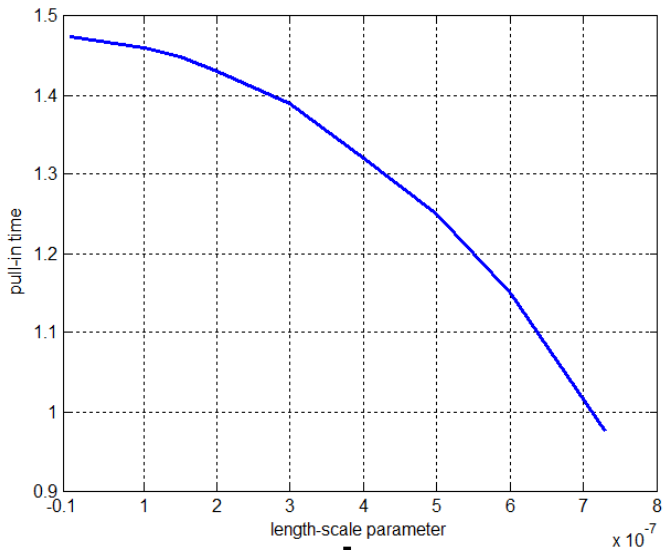

Figure 8: Pull-in time of the diaphragm subjected to the actuating step DC voltage for different length scale parameters.

4.3 Sensitivity (Frequency Response)

Figure 9 represents frequency response in term of magnitude in absence of electrostatic force applying MCST for different length-scale parameters. Increasing the length-scale parameter leads to the

less deflection and the more fundamental frequency. As a result of that the sensitivity in output voltage terms decreases.

As can be seen in figure 10 by increasing the bias DC voltage under constant sound pressure, the deflection increases, So does the sensitivity. In addition, it is evident that the higher bias DC voltages create the lower fundamental frequency which leads to the limitation in the upper band of the frequency response.

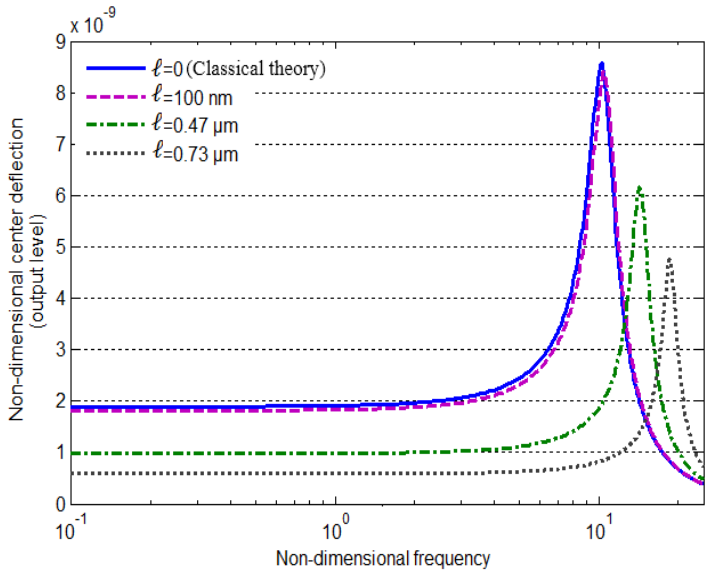

Figure 9: Frequency response of the diaphragm based on modified couple stress theory for different length scale parameters in comparison to the classical theory.

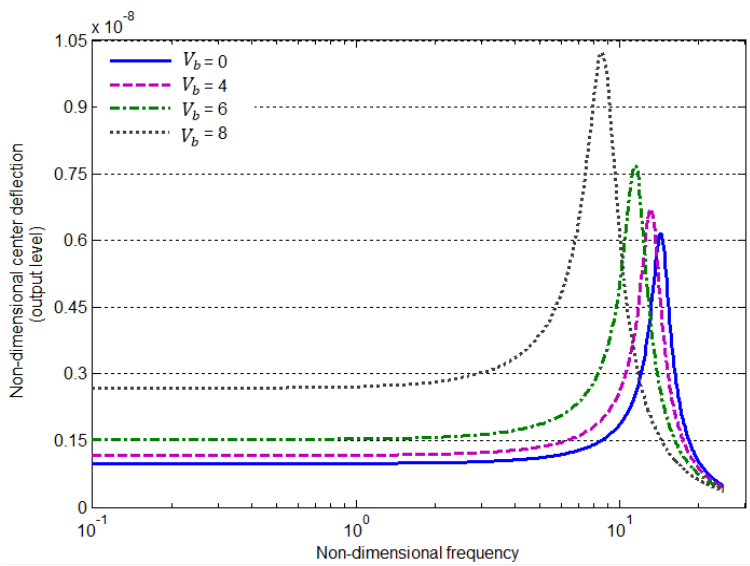

Figure 10: Frequency response of the diaphragm for various bias voltages under modified couple stress theory (ℓ=0.47μm).

5 CONCLUSIONS

This paper studied the size dependent behavior of the capacitive microphone with circular diaphragm using MCST. The numerical results show that the pull-in voltage calculated by modified couple stress theory is more than that calculated by the classical one. It was shown that considering the air damping, the dynamic pull-in voltage escapes from that of obtained by ignoring the damping force and rising damping coefficient has caused the dynamic pull-in voltage to converge to the static pull-in voltage. Also as the length-scale parameter is increased the pull-in time is decreased. Moreover, it is interpreted that under the same condition (the same sound pressure and the same bias voltage) the deflection estimated by the proposed theory is smaller than that by the classical theory. Consequently, the MCST predicts the less output voltage or the less sensitivity in comparison to CT. According to the results, by increasing electrostatic force, the diaphragm deflection is increased and the fundamental frequency is decreased. Therefore, the sensitivity is increased.

The main conclusion to be drawn from this paper is that using the classical theory for diaphragms with considerable material length scale parameter may return inaccurate results and mechanical behavior of the capacitive microphones should be study under modified couple stress theory.

References

Abdel-Rahman, E.M., Younis, M.I., Nayfeh, A.H. (2002). Characterization of the mechanical behavior of an electrically actuated microbeam. Journal of Micromechanics and Microengineering 12: 759–766.

Bao, M., Yeng, H., (2007). Squeeze film air damping in MEMS. Sensors and Actuators A: Physical 136: 3-27.

Batra, R.C., Porfiri, M., Spinello, D. (2006). Analysis of electrostatic MEMS using meshless local Petrov–Galerkin (MLPG) method. Engineering Analysis with Boundary Elements 30: 949–962.

Batra, R.C., Porfiri, M., Spinello, D. (2008). Vibrations and pull-in instabilities of microelectromechanical von Kármán elliptic plates incorporating the Casimir force. Journal of Sound and Vibration 315: 939-960.

Bin, j., Wanji, C., (2010). A new analytical solution of pure bending beam in couple stress elasto-plasticity Theory and applications. International Journal of Solids and Structures 47; 779-785.

Cao, Y., Nankivil, D.D., Allameh, S., Soboyejo, W.O. (2007). Mechanical Properties of Au Films on Silicon Substrates, Materials and Manufacturing Processes 22: 187-194.

Chen, J., Hsu, Y.C., Lee, S.S., Mukherjee, T., Fedder, G.K. (2008). Modeling and simulation of a condenser microphone. *Sensors* and *Actuators* A 145-146: 224-230.

Cosserat, E. and Cosserat, F., (1909). Theorie des Corps Deformables, Hermann et Fils (Paris).

De Silva, C.W. (2005). Vibration and shock handbook, CRC Press (New York).

Eringen, A.C. (1983). On differential equations of nonlocal elasticity and solutions of screw dislocation and surface waves. Journal of Applied Physics 54: 4703–4710.

Ganji, B.A., Majlis, B.Y., (2009). Design and fabrication of a new MEMS capacitive microphone using a perforated alumunum diaphragm. Sensors and Actuators A 149: 29–37.

Josue, E., Rufer, L., Rehder, G. (2011). Capacitive microphone fabricated with CMOS-MEMS surface-micromachining technology. Design, Test, Integration and Packaging of MEMS/MOEMS (DTIP), Symposium on. IEEE.

Kim, H.J., Lee, J.W., Lee, S.K., Park, K.H. (2007). A Miniature Condenser Microphone for Portable Terminals Applications. IEEE Sensors Conference.

Koiter, W.T. (1969). Couple-stresses in the theory of elasticity: I & II. Proc K Ned Akad Wet B 67: 17–44.

Kwon, H.S., Funaki, H., Lee, K.C. (2007). Double-chip condenser microphone for rigid backplate using DRIE and wafer bonding technology. *Sensors* and *Actuators* A 138: 81–86.

Lazopoulos, K.A. (2004). On the gradient strain elasticity theory of plates. *European Journal of Mechanics - A/Solids* 23: 843–852.

Lazopoulos, K.A. (2009). On bending of strain gradient elastic micro-plates. Mechanics Research Communications 36: 777–783.

Li, X., Lin, R., Kek, H., Miao, J., Zou, Q. (2001). Sensitivity-improved silicon condenser microphone with a novel single deeply corrugated diaphragm. *Sensors* and *Actuators* A 92: 257–262.

Ma, H.M., Gao, X.L., Reddy, J.N. (2008). A microstructure-dependent Timoshenko beam model based on a modified couple stress theory. Journal of the Mechanics and Physics of Solids 56: 3379–3391.

Ma, T., Man, T.Y., Chan, Y.C., Zohar, Y., Wong, M. (2002). Design and fabrication of an integrated programmable floating-gate microphone. The Fifteenth IEEE International Conference on Micro Electro Mechanical Systems pp. 288-291.

Miao, J., Lin, R., Chen, L., Zou, Q., Lim, S.Y., Seah, S.H. (2002). Design consideration in micromachined silicon microphones. Microelectronics Journal 33: 21–28

Mindlin, R.D., Tiersten, H.F., (1962). Effects of couple-stresses in linear elasticity. Archive for Rational Mechanics and Analysis 11: 415–448.

Nayfeh, A.H. and Mook, D.T., (1979). Nonlinear Oscillations, Wiley (New York).

Nayfeh, A.H., Younis, M.I., Abdel-Rahman, E.M. (2007). Dynamic pull-in phenomenon in MEMS resonators. Nonlinear Dynamics 48: 153–163.

Osterboerg, P.M. (1995). Electrostatically actuated microelectromechanical test structures for material property measurements, Ph.D. Thesis, MIT, Cambridge.

Park, S.K., Gao, X.L., (2006). Bernoulli–Euler beam model based on a modified couple stress theory. Journal of Micromechanics and Microengineering 16: 2355–2359.

Quaegebeur, N., Chaigne, A., (2008). Nonlinear vibrations of loudspeaker-like structures. Journal of Sound and Vibration 309: 178–196.

Raichel, D.R. (2000). The Science and Applications of Acoustics, Springer (New York).

Reddy, J.N. (2002). Energy Principles and Variational Methods in Applied Mechanics. 2nd edn. Wiley (New York).

Reddy, J.N. (2010). Nonlocal nonlinear formulations for bending of classical and shear deformation theories of beams and plates. *International Journal of Engineering Science* 48: 1507–1518.

Rezazadeh, G., Fathalilou, M., Shabani, R. (2009). Static and dynamic stabilities of a microbeam actuated by a piezoelectric voltage. Microsystem Technologies 15: 1785-1791.

Rezazadeh, G., Keyvani, A., Jafarmadar, S. (2012). On a MEMS based dynamic remote temperature sensor using transverse vibration of a bi-layer micro-cantilever. Measurement journal 45: 580-589.

Rezazadeh, G., Ghanbari, M., Mirzaee, I., Keyvani, A. (2010). On the Modeling of a Piezoelectrically Actuated Microsensor for Simultaneous measurement of Fluids Viscosity and Density. Measurement journal 43: 1516–1524.

Scheeper, P.R., Van der Donk, A.G.H., Olthuis, W., Bergveld, P. (1994). A Review of Silicon Microphones. *Sensors* and *Actuators* A 44: 1-11.

Sun, Y., Tohmyoh, H., (2009). Thermoelastic damping of the axisymmetric vibration of circular plate resonators. Journal of sound and vibration 319: 392-405.

Suzuki, K., Funaki, H., Naruse, Y. (2006). MEMS optical microphones with electro-statically controlled grating diaphragm. Measurement Science and Technology 17: 819–824.

Tilmans, H.A.C., Legtenberg, R., (1994). Electrostatically driven vacuum-encapsulated polysilicon resonators Part II. Theory and performance. *Sensors* and *Actuators* A 45: 67–84.

Toupin, R.A. (1962). Elastic materials with couple-stresses. Arch. Ratio. Mech. Anal. 11:385–414.

Tsiatas, G.C. (2009). A new Kirchhoff plate model based on a modified couple stress theory. International Journal of Solids and Structures 46: 2757-2764.

Vahdat, AS., Rezazadeh, G., Afrang, A. (2011). Improving response of a MEMS capacitive microphone filtering shock noise. Microelectronics Journal 42: 614–621.

Whelan, M.J. and Hodgon, M.J., (1978). Essential Principles of Physics, J.W. Arrowsmith Ltd. (Bristol).

Yang, F., Chong, A.C.M., Lam, D.C.C., Tong, P. (2002). Couple stress based strain gradient theory for elasticity. International Journal of Solids and Structures 39: 2731–2743.